


# Triazole RGD antagonist reverts TGF $\beta$ 1-induced endothelial-to-mesenchymal transition in endothelial precursor cells

Francesca Bianchini<sup>1</sup>  · Silvia Peppicelli<sup>1</sup> · Pierangelo Fabbrizzi<sup>2</sup> · Alessio Biagioni<sup>1</sup> · Benedetta Mazzanti<sup>3</sup> · Gloria Menchi<sup>2,4</sup> · Lido Calorini<sup>1</sup> · Alberto Pupi<sup>1,4</sup> · Andrea Trabocchi<sup>2,4</sup>

Received: 21 June 2016 / Accepted: 8 October 2016 / Published online: 19 October 2016  
© The Author(s) 2016. This article is published with open access at Springerlink.com

**Abstract** Fibrosis is the dramatic consequence of a dys-regulated reparative process in which activated fibroblasts (myofibroblasts) and Transforming Growth Factor  $\beta$ 1 (TGF $\beta$ 1) play a central role. When exposed to TGF $\beta$ 1, fibroblast and epithelial cells differentiate in myofibroblasts; in addition, endothelial cells may undergo endothelial-to-mesenchymal transition (EndoMT) and actively participate to the progression of fibrosis. Recently, the role of  $\alpha$ v integrins, which recognize the Arg-Gly-Asp (RGD) tripeptide, in the release and signal transduction activation of TGF $\beta$ 1 became evident. In this study, we present a class of triazole-derived RGD antagonists that interact with  $\alpha$ v $\beta$ 3 integrin. Above different compounds, the RGD-2 specifically interferes with integrin-dependent TGF $\beta$ 1 EndoMT in Endothelial Colony-Forming Cells (ECFCs) derived from circulating Endothelial Precursor Cells (EPCs). The RGD-2 decreases the amount of membrane-associated TGF $\beta$ 1, and reduces both ALK5/TGF $\beta$ 1 type I receptor expression and Smad2 phosphorylation in ECFCs. We found that RGD-2 antagonist reverts EndoMT, reducing  $\alpha$ -smooth muscle actin ( $\alpha$ -SMA) and vimentin

expression in differentiated ECFCs. Our results outline the critical role of integrin in fibrosis progression and account for the opportunity of using integrins as target for anti-fibrotic therapeutic treatment.

**Keywords**  $\alpha$ v $\beta$ 3 integrin · Endothelial Colony-Forming Cells (ECFCs) · Endothelial-to-Mesenchymal Transition (EMT) · Fibrosis · Transforming Growth Factor $\beta$ 1 (TGF $\beta$ 1)

## Abbreviations

ALK	Activin receptor-Like Kinase
$\alpha$ -SMA	Alpha-Smooth Muscle Actin
$\alpha$ v $\beta$ 3	Alphavbeta3 integrin
ECFC	Endothelial colony-forming cells
ECM	Extracellular matrix
EndoMT	Endothelial-to-mesenchymal transition
ERK1/2	Extracellular signal-regulated kinases 1/2
FN	Fibronectin
MEndoT	Mesenchymal-to-endothelial transition
RGD	Arginine-glycine-aspartic acid
OPN	Osteopontin
Smad	Small mothers against decapentaplegic homolog
TGF- $\beta$	Transforming growth factor- $\beta$
VN	Vitronectin

## Introduction

Fibrotic disease encloses a wide array of different pathologies both systemic such as systemic sclerosis (SSc) and sclerodermatous graft versus host disease (Scl GVHD), and organ-specific pathologies as idiopathic pulmonary fibrosis (IPF), liver cirrhosis, and progressive kidney

✉ Francesca Bianchini  
francesca.bianchini@unifi.it

<sup>1</sup> Department of Clinical and Experimental Biomedical Science “Mario Serio”, University of Florence, Florence, Italy  
<sup>2</sup> Department of Chemistry “Ugo Schiff”, University of Florence, Florence, Italy  
<sup>3</sup> Cord Blood Bank, Careggi University Hospital, Florence, Italy  
<sup>4</sup> Interdepartmental Center for Preclinical Development of Molecular Imaging (CISPIM), University of Florence, Florence, Italy

disease. Although the etiology of these fibrotic disorders remains unexplained and may vary from disease to disease, the common pathogenetic signs are the deposition of extracellular matrix (ECM) synthesized by activated myofibroblasts and the persistence of inflammation [1, 2]. High levels of cytokines, growth factors, and proteolytic enzymes produced by activated macrophages and lymphocytes restrain the resolution process and fibrosis expands gradually. Finally, matrix deposition rearranges the tissue architecture, causing organ failure and patient death. Thus, fibrotic diseases in their complex are life-threatening diseases recognized to represent an important health issue [3].

Transforming growth factor $\beta$ 1 (TGF $\beta$ 1) has been identified as the most important mediator in many types of tissue fibrosis [4]. TGF $\beta$ 1 induces fibroblasts differentiation into myofibroblasts providing collagen and ECM protein deposition [5]. Experimental studies have provided evidences that myofibroblasts not only originate from resident fibroblasts, but also derive from the transdifferentiation of epithelial cells, endothelial cells, and bone marrow-derived cells [6, 7]. Endothelial cells and bone marrow-derived endothelial cells, when exposed to TGF $\beta$ 1, undergo endothelial–mesenchymal transition (EndoMT). As a consequence, endothelial cells lose their biological characteristic of the endothelial phenotype, acquire typical mesenchymal features, and concurrently express typical markers of myofibroblastic differentiation:  $\alpha$ -smooth muscle actin ( $\alpha$ -SMA), vimentin, and collagen production [8].

TGF $\beta$ 1 is produced as inactive pro-peptide by different types of inflammatory cells. The mature cytokine is exposed in the extracellular space non-covalently associated to a latency-associated peptide (LAP), and the LAP–TGF $\beta$ 1 pro-peptide forms a homodimer complex. This complex, which prevents the interaction of the mature cytokine with its receptors, is stored in the extracellular space, closely associated to the cell membrane and bounded to specific latent TGF $\beta$ 1 binding proteins (LTBP). LTBP fixes the system in association to fibrillin-1 and fibronectin. The release of the non-covalently bounded mature TGF $\beta$ 1 from the LAP complex occurs by the action of proteases (matrix metalloproteases MMP, thrombin, and plasmin) or by the effect of environmental condition changes (pH, pO<sub>2</sub>, or temperature) [9, 10]. Moreover, in the recent years, the role of  $\alpha$ v integrins in TGF $\beta$ 1 release from the LAP complex during fibrotic disease progression became evident [11, 12]. It has been demonstrated that  $\alpha$ v integrins recognize the tripeptide Arg-Gly-Asp (RGD) sequence of the LAP, and the integrin binding induces a stretch of the complex and a mechanical release of the active TGF $\beta$ 1 [13]. In addition, it is known that  $\alpha$ v integrins might function as docking site for MMPs contributing

to the protease-dependent release of TGF $\beta$ 1. Thus, the maintenance of high levels of TGF $\beta$ 1 exacerbates tissue damages and outlines the important role of integrins in the instauration and progression of fibrosis [14, 15].

In this study, we present a novel class of  $\alpha$ v $\beta$ 3 RGD antagonists that interfere with integrin-dependent release of TGF $\beta$ 1 from LTBP complex. Interestingly, we found that the RGD-2-integrin antagonist counteracts the TGF $\beta$ 1-induced myofibroblast differentiation of endothelial precursor cells (ECPCs) by interfering, in these cells, with the autocrine loop of TGF $\beta$ 1 activation.

These findings may suggest an innovation in anti-fibrotic treatment. The common anti-fibrotic treatments are based, so far, on the use of corticosteroids and immunosuppressant drugs. These drugs may retard, but do not arrest, the disease progression. Thus, the cooperation between anti-fibrotic available drugs and novel RGD antagonists might contribute to the inhibition of the vicious cycle, led by TGF $\beta$ 1, underlying the disease progression.

## Results

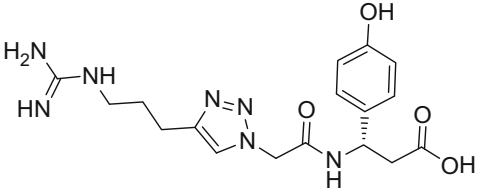
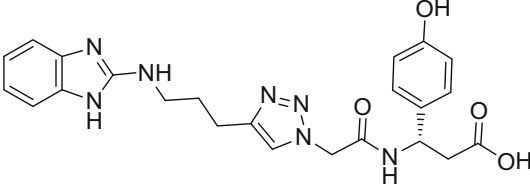
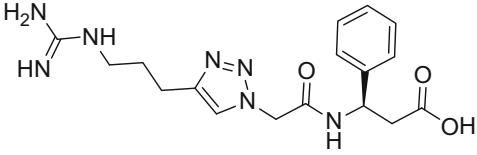
### RGD triazole-derived $\alpha$ v $\beta$ 3 antagonists

RGD triazole-derived antagonists of the  $\alpha$ v $\beta$ 3 integrin receptor were synthesized in our laboratory as previously described [16]. Solid-phase assay was used to test the ability of RGD ligands to compete with <sup>125</sup>I-echistatin for the binding to  $\alpha$ v $\beta$ 3 integrin receptor. We found that RGD-1 compound showed an IC<sub>50</sub> value of  $2.1 \pm 1.3 \mu\text{M}$ , while compound RGD-2 showed an IC<sub>50</sub> of  $37 \pm 11 \text{ nM}$ . In contrast, the IC<sub>50</sub> value of RGD-3 compound was found to be  $>10 \mu\text{M}$ , addressing for a less active antagonistic efficacy toward  $\alpha$ v $\beta$ 3 receptor (Table 1).

### Effect of the triazole RGD antagonists on ECPCs adhesion

ECPCs, isolated from human umbilical cord blood (UCB), were characterized using flow cytometry assay by surface expression of endothelial cell-specific antigens: Ulex europaeus I agglutinin (Ulex), Platelet Endothelial Cell Adhesion Molecule-1 (PECAM-1/CD31), Vascular Endothelial Growth Factor Receptor 2 (VEGFR-2/KDR), Phagocytic Glycoprotein-1 (CD44), integrin  $\beta$ 1-chain (CD29), and integrin heterodimers  $\alpha$ v $\beta$ 3 (Fig. 1a). ECPCs were monitored throughout the experimental procedures for  $\alpha$ v $\beta$ 3 integrin expression (Fig. 1b), the maintenance of endothelial phenotype (Fig. 1c), and the in vitro tube formation ability (Fig. 1d). Sub-confluent cultures of ECPCs between the 3rd and 6th passage were exposed to different doses (10, 1, 0.1, and 0.01  $\mu\text{M}$ ) of three different triazole

**Table 1** Inhibition of  $^{125}\text{I}$ -echistatin-specific binding to purified human integrin proteins  $\alpha\text{v}\beta_3$  by triazole-containing RGD peptidomimetics

Triazole-derived RGD antagonist	Structure	Specific binding versus $\alpha\text{v}\beta_3$ , IC <sub>50</sub> ( $\mu\text{M}$ )
RGD-1 <sup>16</sup>		$2.1 \pm 1.3$
RGD-2 <sup>16</sup>		$0.037 \pm 0.011$
RGD-3 <sup>18</sup>		$>10$

RGD antagonists and allowed to adhere to vitronectin (VN) for 1 h. At the end of the incubation, non-adherent cells were removed by a gentle wash with PBS. We found a 40 % of inhibition of ECPCs adhesion to VN for RGD-1 compound at 10  $\mu\text{M}$ , whereas lower concentrations of this compound showed a weak inhibition of cells adhesion. The RGD-2 compound clearly inhibited ECPCs adhesion to VN in a dose-dependent manner, ranging from 80 % of inhibition at 10  $\mu\text{M}$  to 20 % at 10 nM. Finally, RGD-3 compound did not significantly inhibit ECPCs adhesion to VN (Fig. 1e). To further evaluate RGD-2 inhibitory activity toward different RGD containing substrata, ECPCs cells were exposed to RGD-2 compound at different doses before adhesion to osteopontin (OPN), Fibronectin (FN), and Matrigel. We found that RGD-2 antagonist showed a dose-dependent inhibition of ECPCs adhesion to OPN from 75 % at 10  $\mu\text{M}$  to 25 % at 10 nM. In contrast to this, inhibition of adhesion to FN and Matrigel was very weak. Matrigel was used as negative control since it is composed by laminin, collagen IV, nidogen/enactin, and proteoglycan, which are ligands for other non-RGD families of integrin receptors (laminin-type and collagen-type) (Fig. 1f).

#### Effect of RGD-2 triazole compound on $\alpha\text{v}\beta_3$ expression in TGF $\beta$ 1-stimulated ECPCs

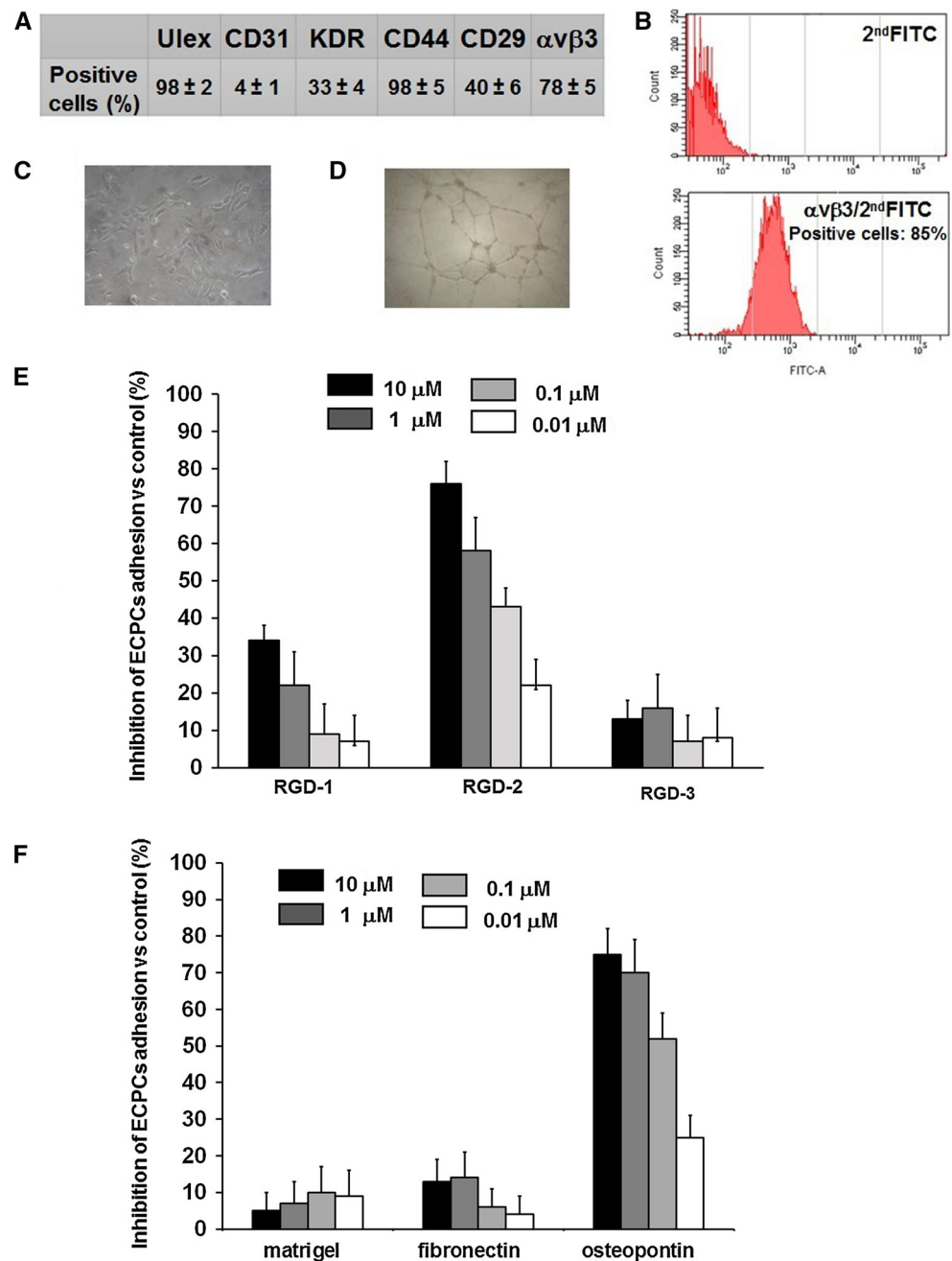
ECPCs were exposed to RGD-2 compound at 1  $\mu\text{M}$  and/or TGF $\beta$ 1 at 1 nM/ml for 24 h. Here we found an

overexpression of  $\beta_3$  subunit mRNA in TGF $\beta$ 1-treated ECPCs, while the co-treatment with the RGD-2 antagonist did not show any  $\beta_3$  subunit increase (Fig. 2a). Along with this, we found that protein expression of  $\alpha\text{v}\beta_3$  receptor was increased, in TGF $\beta$ 1 treated ECPCs, while treatment with RGD-2 antagonist abrogates TGF $\beta$ 1, inducing  $\alpha\text{v}\beta_3$  expression in ECPCs (Fig. 2b).

#### Effect of RGD-2 antagonist on TGF $\beta$ 1 signal transduction pathway and TGF $\beta$ 1 expression on ECPCs cell membrane

In order to evaluate the signal transduction activation of TGF $\beta$ 1 pathway in ECPCs cells, we investigated ALK-5 expression and SMAD phosphorylation after TGF $\beta$ 1 and/or RGD-2 treatment. We observed that 24 h treatment with TGF $\beta$ 1 induces the increase of ALK-5 expression also in the presence of the RGD antagonist (Fig. 3a). Moreover, when we evaluated SMAD2 phosphorylation, we found an increase in Phospho-SMAD2 in TGF $\beta$ 1-treated cells, while in RGD-2/TGF $\beta$ 1-co-treated cells, SMAD2 phosphorylation was similar to untreated cells (Fig. 3b). We, also, evaluated the effect of RGD-2 antagonist on TGF $\beta$ 1 activation in ECPCs. Cells were exposed for 24 h to exogenous TGF $\beta$ 1 (1 ng/ml). After the removal of the medium, cells were allowed to grow for the next 24 h in a standard medium. At the end of the second incubation, ECPCs were lysed directly in tissue culture plates and processed for western blotting analysis. We found high levels of

**Fig. 1** RGD triazole-derived antagonists on ECPCs adhesion to RGD containing substrata. **a** Flow cytometric analysis of surface antigens expression in freshly isolated ECPCs (percentage of positive cells). **b** flow cytometric analysis of  $\alpha v\beta 3$  integrin expression of cultured cells, **c** contrast microscopy images of ECPCs growing cultures, and **d** contrast microscopy images of ECPCs tube formation. **e** Inhibition of adhesion of ECPCs to VN in the presence of different concentration of different RGD triazole antagonists (RGD-1, RGD-2, and RGD-2 triazole compounds), and **f** inhibition of adhesion of ECPCs to Matrigel, FN, and OPN in the presence of different concentrations of RGD-2 antagonist. Representative results from three different experiments. Values represent the mean  $\pm$  SD



membrane-associated TGF $\beta$ 1, in TGF $\beta$ 1-treated cells, compared to untreated cells. While the treatment with RGD-2 antagonist (1  $\mu$ M) alone did not modify TGF $\beta$ 1 levels, the co-treatment with TGF $\beta$ 1 and RGD-2 antagonist reduced significantly the expression of endogenous TGF $\beta$ 1 to the levels found in untreated cells (Fig. 3a).

#### RGD-2 antagonist reverts TGF $\beta$ 1-induced EndoMT in ECPCs

We found that TGF $\beta$ 1 significantly increased the expression of  $\alpha$ -SMA and vimentin in ECPCs together with a

significant switch to an elongated morphology. Upon the morphological observation of ECPC-treated cultures, we found that TGF $\beta$ 1-treated cells present a fibroblast-like morphology, as expected, but this change was absent when the cells were treated with the RGD antagonist and TGF $\beta$ 1, and the culture morphology was slightly similar to that of untreated cells (Fig. 4a). RGD-2 antagonist-treated cells express  $\alpha$ -SMA and vimentin at levels similar to the untreated cells. Thus, the treatment with the RGD-2 antagonist in association with TGF $\beta$ 1 significantly reduced the expression of mesenchymal markers of EndoMT, as demonstrated in western blotting analysis and in

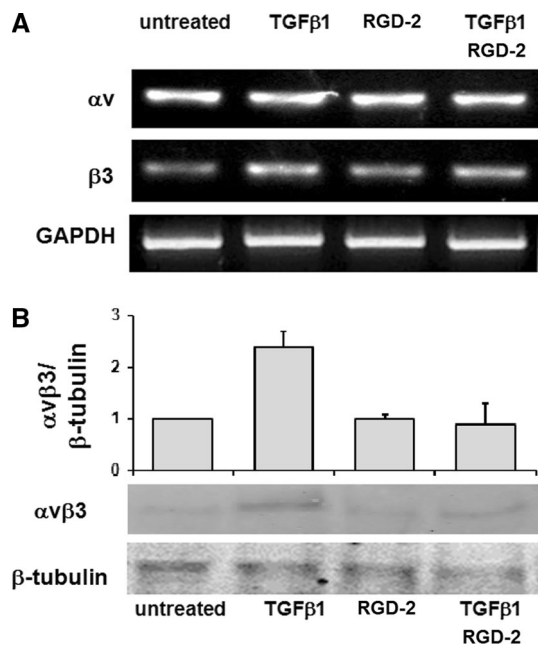


**Fig. 2** Effect of RGD-2 on  $\alpha v\beta 3$  expression in ECPCs. Integrin  $\alpha v\beta 3$  expression in ECPCs after 24 h treatment with exogenous TGF $\beta 1$  (1 ng/ml) and/or 1  $\mu$ M RGD-2 antagonist: **a** mRNA for  $\alpha v$ ,  $\beta 3$  subunits, and GAPDH, and **b**  $\alpha v\beta 3$  protein expression and densitometric analysis

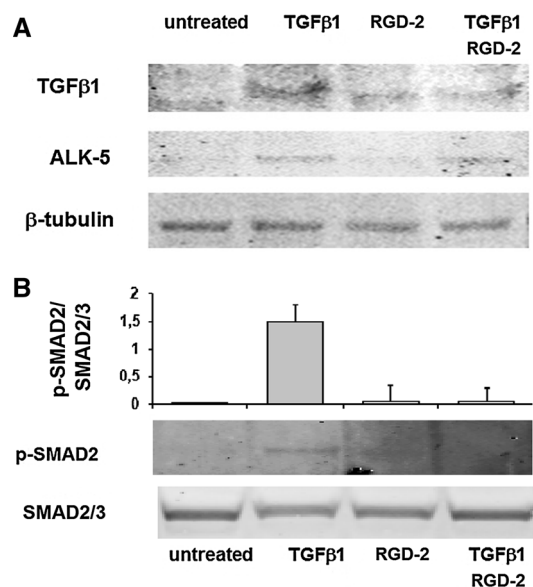


**Fig. 3** Effect of RGD-2 antagonist on TGF $\beta 1$  signal transduction pathway and TGF $\beta 1$  expression on ECPCs cell membrane. **a** TGF $\beta 1$  and ALK-5 were evaluated in ECPCs exposed for 24 h to exogenous TGF $\beta 1$  and/or RGD-2 triazole and for additional 24 h to fresh standard medium. **b** Protein expression and densitometric analysis of PhosphoSMAD2 (pSMAD2) evaluated in ECPCs exposed to exogenous TGF $\beta 1$  and/or RGD-2 for 1 h. All experiments were conducted at least three times. Values represent the mean  $\pm$  SD. \* $P < 0.05$

immunofluorescence (Fig. 4b). Next, we evaluated MAPK pathway activation after exposure to TGF $\beta 1$  and to the co-treatment TGF $\beta 1$ /RGD-2. We found that ERK1/2

phosphorylation increases in ECPCs after treatment with exogenous TGF $\beta 1$ , and that the co-treatment with TGF $\beta 1$ /RGD-2 inhibited ERK1/2 phosphorylation (Fig. 4c). To explore the effect of RGD antagonist on ECPCs biological behavior during TGF $\beta 1$ -induced EndoMT, we evaluated the invasive activity, wound healing ability, and in vitro angiogenesis of cells exposed to exogenous TGF $\beta 1$  and RGD-2 antagonist. We found a significant reduction in ECPCs invasion through Matrigel after treatment with exogenous TGF $\beta 1$ . Significant but less intense reduction in ECPCs invasion was found after treatment with RGD-2 antagonist alone, while the treatment with RGD antagonist together with TGF $\beta 1$  partially restored the originally migratory phenotype of the cells (Fig. 4d). Moreover, it is widely recognized that ECPCs exert a fundamental role the healing process, restoring the physiological function of vascular network. We found that, accordingly with previous finding, ECPCs cells exposed to TGF $\beta 1$  lose their wound healing potency, while ECPCs cells treated with TGF $\beta 1$  and RGD-2 antagonist almost completely recover their ability to heal the wound. Finally, it is known that ECPCs are characterized by their high proliferation rate and by their ability to give rise to capillary network in the in vitro angiogenic assay; thus, ECPCs were seeded on Matrigel in the presence of TGF $\beta 1$  and/or the RGD-2 antagonist. After 24 h incubation, the number of branches per field was counted. We observed a significant decrease in the number of branches of ECPCs treated with TGF $\beta 1$  as compared to untreated cells. The co-treatment with the RGD antagonist partially restored the ECPCs ability to form a capillary network (Fig. 4f).

## Discussion

In the present study, we investigated the role of different triazole-derived RGD antagonists in the TGF $\beta 1$  loop of ECPCs activation during endothelial–mesenchymal transition (EndoMT). Above the different triazole-derived compounds, we found that the stereochemistry of the tyrosine/phenyl moiety was crucial for the antagonistic efficiency of the compounds. The guanidine substitution, in the arginine mimetic portion of the molecule with the aminopyridine moiety, increased the binding affinity toward  $\alpha v\beta 3$  integrin. Integrin  $\alpha v\beta 3$  specifically recognizes the Arg-Gly-Asp (RGD) tripeptide present in the sequence of different extracellular matrix proteins. Although ECPCs express the integrin receptors  $\alpha v\beta 3$  and  $\alpha 5\beta 1$  which recognize RGD extracellular matrix proteins as vitronectin (VN), fibronectin (FN), and osteopontin (OPN), in our conditions, ECPCs adhesion to FN was not inhibited by the RGD antagonist; this result might be explained outlining two observations. The first is that  $\alpha v\beta 3$  and  $\alpha 5\beta 1$ , even

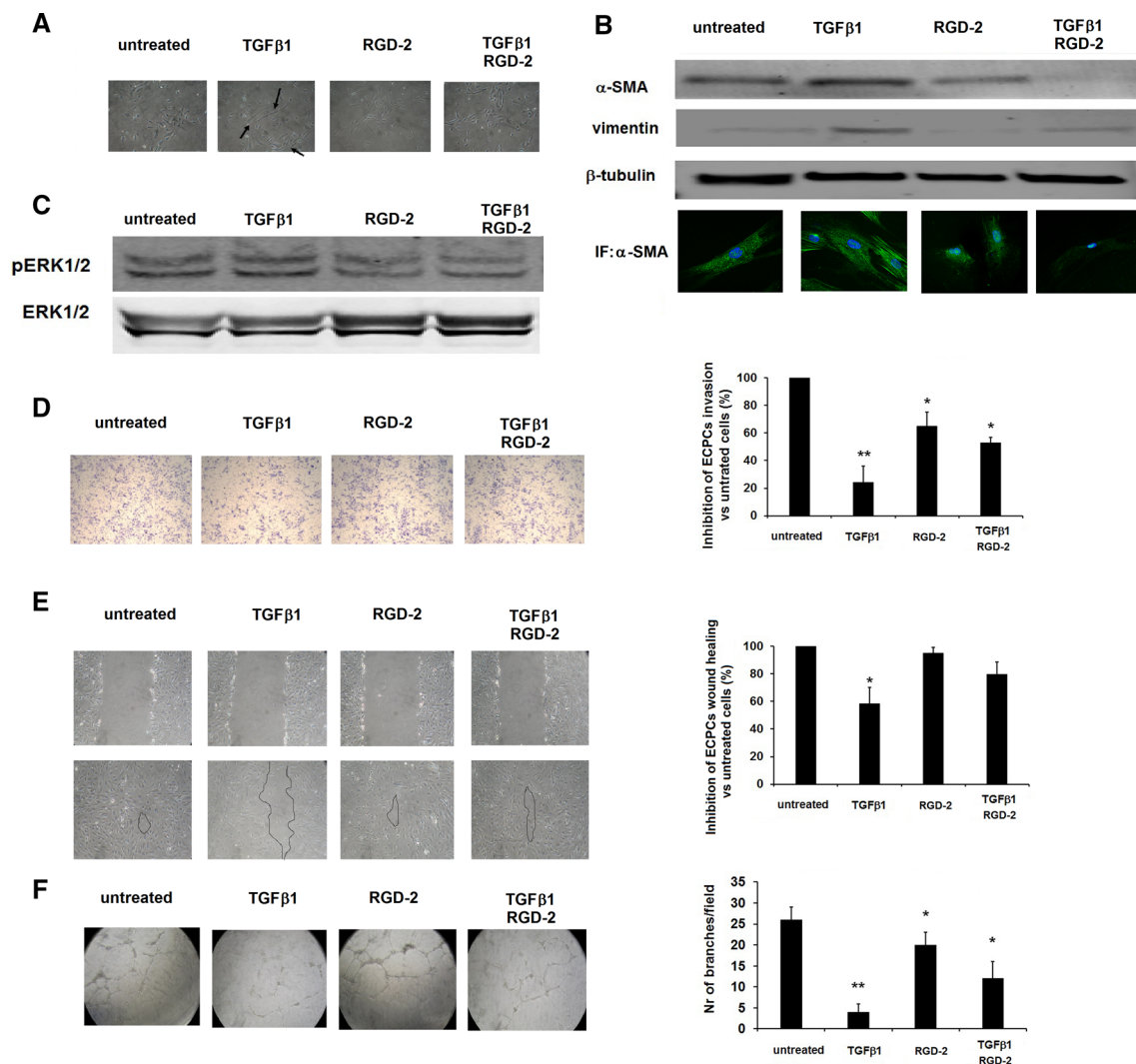


**Fig. 4** RGD-2 antagonist reverts TGFβ1-induced EndoMT in ECPCs. **a** Contrast microscopy representative images of ECPCs after 24 h treatment with TGFβ1 and/or RGD-2 compound, morphological changes. **b** Expression of EndoMT markers of mesenchymal differentiation; ECPCs were exposed to exogenous TGFβ1 (1 ng/ml) and/or 1 μM RGD-2 antagonist for 24 h, and α-SMA and vimentin expression were evaluated. *Upper panel*: western blotting for α-SMA and vimentin; *lower panel*: representative immunofluorescence images for α-SMA. **c** TGFβ1-induced phosphoERK1/2 activation, ECPCs were exposed to different treatments for 24 h and lysed. **d** Invasiveness through Matrigel of ECPCs after 24 h treatment with exogenous TGFβ1 (1 ng/ml) and/or 1 μM RGD-2 antagonist; for quantification, migrated cells were counted in six randomly chosen

fields for each filter. **e** Wound healing assay of ECPCs after 24 h treatment with exogenous TGFβ1 (1 ng/ml) and/or 1 μM RGD-2 antagonist; the degree of healing was quantified by measuring the distance between opposing edges of the wound. Four wound/treatment and three measurements/wound were taken. **f** In vitro tube formation of ECPCs after 12 h treatment with exogenous TGFβ1 (1 ng/ml) and/or 1 μM RGD-2 antagonist; for quantification, the number of branches per field was evaluated at 40 magnifications, in four different fields. Data were obtained from three independent experiments. Percentage of inhibition was expressed compared to untreated cells. Values represent the mean ± SD. \* $P < 0.05$ , \*\* $P < 0.01$

though recognize the RGD tripeptide sequence, display specific binding affinity for a given ligand depending also on few essential amino acid residues surrounding the binding site pocket of the integrin receptor itself; thus, VN and OPN exhibit higher binding affinity for αvβ3 integrin, while FN exhibits high binding affinity to α5β1 integrin [17]. The second observation is that different RGD antagonist might display a different affinity to the same integrin

receptor depending on those interactions with receptor amino acid residues close to the binding pocket [18].

Many clinical and experimental observations confirm the key role of TGFβ during the instauration and the persistence of the fibrotic disease, mostly through the auto-crine loop of TGFβ activation [19]. The TGFβ belongs to a ligand superfamily comprising the three forms of TGFβs (TGFβ1, TGFβ2, and TGFβ3), Activins, BMPs (Bone

Morphogenetic Proteins), and GDFs (Growth and Differentiation Factors). In general, TGF $\beta$  superfamily ligands bind to a complex of TGF $\beta$  type I and TGF $\beta$  type II serine/threonine kinase receptors. In the absence of stimuli, the homodimers of type I, also known as Activin receptor-Like Kinase (ALK), and of type II receptors are expressed on the cell surface in a separate form [20].

Upon recognition of the TGF $\beta$ 1 by the type II receptor, whose function is to present the ligand, the activation of the downstream signal requires the association of the type I/type II receptors in a heterotetrameric complex and the transphosphorylation of the type I receptor/ALK by the serine/threonine kinase activity of type II receptor. Then, the type I receptor transfers the signal into the nucleus by the phosphorylation of the SMAD proteins. The combination of different type II/type I tetrameric receptors determines the activation of different downstream signaling pathways, in response to the same ligand [21].

In endothelial cells, soluble TGF $\beta$ 1 interacts with type II receptor (TGF $\beta$ 1RII) and, among the different types of ALKs, ALK-5 phosphorylation induces the activation of SMAD2/3 pathway involved in endothelial cells inhibition of proliferation/migration and in the promotion of the extracellular matrix proteins synthesis, while ALK-1 phosphorylation induces the activation of SMAD1 and SMAD5 pathways that leads to endothelial cells migration and proliferation [22].

ECPCs might contribute substantially to the overexpression of TGF $\beta$  that forces the maintenance of a dysregulated reparative process [23]. Thus, it has been demonstrated, in lung fibroblasts, that TGF $\beta$ 1 induces overexpression of  $\alpha$ v $\beta$ 3 integrin which potentiates TGF $\beta$ 1 responsiveness of the cells [24]. Although our findings are not completely exhaustive, indicate that ALK-5 expression is upregulated by exogenous TGF $\beta$ 1 treatment, but that the downstream activation of signal transduction, through the ALK-5 receptor, may depend on  $\alpha$ v $\beta$ 3-mediated release of endogenous TGF $\beta$ 1. Moreover, it is known that the type I receptor, in addition to Smad 2/3 protein phosphorylation, activates other non-Smad signaling pathways involving ERK1/2, TGF- $\beta$ -activated kinase-1 (TAK-1), JNK, p38, Rho GTPases, and the PI3 K-AKT pathways [25]. We observed that while the interaction between the RGD antagonist and the integrin receptor did not induce any downstream signal transduction activation, the co-treatment with triazole RGD antagonist reduced significantly the ERK1/2 activation induced by TGF $\beta$ 1.

TGF $\beta$ 1, being the most important mediator in tissue fibrosis, is recognized to induce in vitro the endothelial-mesenchymal transition in endothelial cells and circulating endothelial precursor cells [26–29]. Despite other authors demonstrated that a cyclic RGD antagonist enhances

in vitro and in vivo vascularization in a model of EPCs [30], we found a mild but significant reduction in the capillary formation after the treatment with the triazole RGD antagonist. This result was in agreement with our previous observation on mature human umbilical vein endothelial cells (HUVEC) [31]. We suggest that our findings depend by the contribution of two main different mechanisms of interaction between the RGD-2 antagonist and the  $\alpha$ v $\beta$ 3 receptor. The first is the direct role that integrin  $\alpha$ v $\beta$ 3 exerts in endothelial cells invasion and in vitro angiogenesis, resulting in a reduction in invasion and angiogenesis operated by the linear triazole peptidomimetic antagonists alone. The second is the interfering effect of RGD-2 antagonist in the TGF $\beta$ 1/ $\alpha$ v $\beta$ 3 crosstalk that reverts EndoMT in ECPCs and exerts a fundamental anti-fibrotic and pro-resolution effect. It has to be noted that the interest in the synthesis and identification of bioactive RGD antagonists originates from the need in improving anti-angiogenic treatment of cancer, since the outcomes of drugs against vascular endothelial growth factor and relative receptors have shown a partial lack of efficacy both in vitro and in vivo [32–34]. The  $\alpha$ v RGD mimetic cyclic pentapeptide, Cilengitide (EMD 121974), has been identified as the first synthesized anti-angiogenic small molecule, and its effect on endothelial cells has been demonstrated [35]. Cilengitide showed encouraging activity in patients with glioblastoma and melanoma, and is currently used in clinical trials [36, 37]. In contrast to this, other authors found that Cilengitide enhances angiogenesis, and promotes tumor growth and cell invasion [38]. In our model, despite the strong effect of the RGD triazole on the inhibition of cell adhesion, we found a weak effect on the inhibition of invasion and angiogenesis that might be explained by the specific and unique activity of this linear triazole RGD antagonist against the  $\alpha$ v $\beta$ 3 receptor. Along with this, we should take into account that invasiveness and tube formation assays are performed on Matrigel substrate, against which the RGD triazole effect is not specific, and that the spatial occupation of the integrin receptor binding site by the RGD triazole may not be sufficient to overcome integrin redundancy in invasiveness and tube formation processes. Indeed, during the ECPCs invasion and migration process, many interactions between ECM and other integrin receptors, as  $\alpha$ 5 $\beta$ 1 and  $\alpha$ 6 $\beta$ 1, have been found to be involved [39–41], as well as many interactions between ECM and cell-derived proteases. Thus, the  $\alpha$ v $\beta$ 3 integrin receptor activity might be only partially involved in ECPCs invasion and tube formation [42].

In a fibrotic lesion, TGF $\beta$ 1 is released by activated fibroblasts and macrophages, or endothelial cells themselves, and induces a local overload of TGF $\beta$ 1 driving to stroma activation. Circulating precursor endothelial cells,

recruited by pro-inflammatory cytokines, differentiate in activated fibroblasts, and endogenous TGF $\beta$ 1 amplifies the fibrotic vicious circle. To date, the therapeutic interventions on fibrotic diseases are the use of anti-inflammatory mediators, immunomodulatory drugs, or agents that directly block TGF $\beta$ 1 activity, such as specific antibody. Unfortunately, anti-inflammatory treatment only retards but does not resolve fibrosis, while TGF $\beta$ 1 antibody might compromise important activity of this cytokine in other tissues [43]. Our findings are in agreement with the importance of integrin involvement in fibrosis [44, 45]. Here, we introduced a new synthesized non-peptidic compound with anti-fibrotic properties in an in vitro model of tissue fibrosis. This RGD antagonist not only prevents the  $\alpha$ v $\beta$ 3-mediated TGF $\beta$ 1 release dampening the autocrine loop of ECPCs activation, but also promotes a mesenchymal-to-endothelial transition (MEndoT), reverting the TGF $\beta$ 1-mediated phenotype of activated endothelial cells. It should be noted that a  $\alpha$ v $\beta$ 6 monoclonal antibody is involved in a phase 2 study for idiopathic pulmonary fibrosis (STX-100, NCT01371035) [46]. This observation confirms the need of further investigations to delineate the role that integrin antagonists might have in the designing of anti-fibrotic therapies. On the whole, our results might support the hypothesis for an EndoMT reversion mediated by RGD antagonist. Exogenous TGF $\beta$ 1, released in the fibrotic microenvironment, induces  $\alpha$ v $\beta$ 3 receptor overexpression in ECPCs. The presence of high levels of  $\alpha$ v $\beta$ 3 receptors enhances the release of active TGF $\beta$ 1 from LAP. Endogenous ECPCs-derived TGF $\beta$ 1 interacts with its receptors on ECPCs themselves promoting EndoMT (Fig. 5a). The RGD antagonist, by occupying the binding site of the  $\alpha$ v $\beta$ 3 receptor, reduces the traction exerted by the heterodimer on the RGD sequence of the LAP, thus reducing endogenous TGF $\beta$ 1 release and dampening the autocrine loop of TGF $\beta$ 1 activation (Fig. 5b).

## Materials and methods

### Synthesis of triazole-based non-peptide RGD peptidomimetic

The triazole-based RGD ligand was achieved using the click chemistry by combining azide and alkyne in the Cu-catalyzed azide–alkyne cycloaddition, followed by acid-mediated hydrolysis of the protecting groups of side chain isosteres [16, 31, 47]. Three bioactive compounds were selected starting from a group of  $\alpha$ v $\beta$ 3 integrin ligands.

### Solid-phase integrin binding assay

The inhibition of  $^{125}$ I-echistatin-specific binding to  $\alpha$ v $\beta$ 3 integrins by RGD antagonists was evaluated as previously reported [47]. Briefly,  $^{125}$ I-echistatin with a specific activity of 2000 Ci/mmol was purchased from Perkin Elmer, and integrin  $\alpha$ v $\beta$ 3 from human placenta was purchased from Millipore. Purified  $\alpha$ v $\beta$ 3 integrin (Millipore) was diluted in coating buffer [20 mM Tris (pH 7.4), 150 mM NaCl, 2 mM CaCl<sub>2</sub>, 1 mM MgCl<sub>2</sub>, 1 mM MnCl<sub>2</sub>] at concentrations of 500 or 1000 ng/mL. Aliquots of  $\alpha$ v $\beta$ 3 integrin (100  $\mu$ L/well) were added to a 96-well plate (Perkin Elmer), and plates were incubated overnight at 4 °C, followed by washings with blocking/binding buffer [20 mM Tris (pH 7.4), 150 mM NaCl, 2 mM CaCl<sub>2</sub>, 1 mM MgCl<sub>2</sub>, 1 mM MnCl<sub>2</sub>, and 1 % BSA], and then incubated at room temperature for an additional 2 h. After two washings with the same buffer, aliquots of  $^{125}$ I-echistatin (0.05 nM) were added to each well with different concentrations of RGD compounds (from 0.01 to 100 nM). Non-specific binding was defined as  $^{125}$ I-echistatin bound in the presence of an excess (1  $\mu$ M) of unlabeled echistatin. After 3 h incubation at RT, plates were washed three times with blocking/binding buffer and counted in a Top-Count NXT microplate scintillation counter (Perkin Elmer) using 200  $\mu$ L/

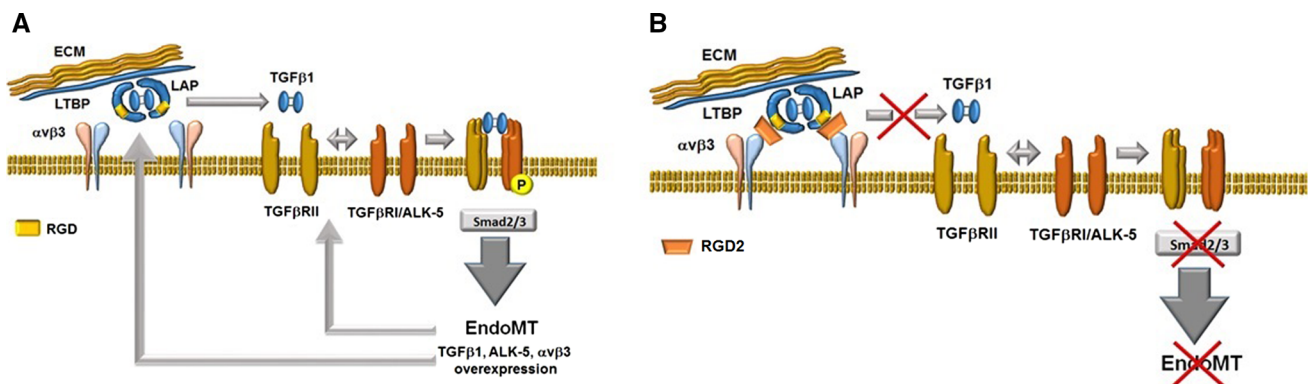


**Fig. 5** Hypothesis for molecular mechanism of RGD antagonist EndoMT reversion in ECPCs. **a** Mechanism of TGF $\beta$ 1-induced EndoMT and  $\alpha$ v $\beta$ 3-mediated autocrine loop of TGF $\beta$ 1 release in

ECPCs. **b** Role of RGD-2 triazole antagonist in dampening autocrine loop of TGF $\beta$ 1 activation



well of MicroScint-40 liquid scintillation (Perkin Elmer). Data are shown as mean  $\pm$  SD from three independent experiments. IC<sub>50</sub> values were determined by fitting binding inhibition data by non-linear regression using GraphPad Prism 4.0 Software Package (GraphPad Prism, San Diego, CA).

### Isolation of endothelial colony-forming cells and culture conditions

Endothelial Colony-Forming Cells (ECPCs), a subpopulation of Endothelial Precursor Cells (EPCs), were isolated from >50 ml human umbilical cord blood (UCB) of health newborns, as described [48, 49], for the banking established by the Umbilical Cord Bank of Careggi Hospital (Florence, Italy) after maternal informed consent in accordance with the Declaration of Helsinki and in compliance with Italian legislation. ECPCs were analyzed for the expression of surface antigens (CD31, CD44, CD29, ULEX, KDR, and  $\alpha v\beta 3$ ) and were grown in complete EGM<sup>TM</sup>-2 BulletKit<sup>TM</sup> (CC-3162 Lonza) with 10 % Fetal Bovine serum (FBS) (Hyclone). Confluent cell cultures were propagated every 3 days, for no more than 10 passage, and seeded on gelatin-coated tissue culture plates at a density of  $5 \times 10^5$  cells/cm<sup>2</sup> in a 5 % CO<sub>2</sub> humidified incubator at 37 °C. ECPCs cultures, grown to subconfluence, were treated for 24 h with 1 ng/mL of hrTGF $\beta$ 1 (Peprotech), or triazole RGD antagonist (1  $\mu$ M), or both in EGM-2 medium (Endothelial cells Growth Medium-2) in the absence of growth factors and in the presence of 2 % FBS (Fetal Bovine Serum). In some experiments, treated cells were exposed to fresh medium for an additional 24 h treatment before protein extraction.

### Flow cytometric analysis

Cells were collected using Accutase (a trypsin-free cell dissociation buffer from Sigma) and resuspended in PBS with 1 % BSA (FACS buffer). After blocking, cells were incubated with 1  $\mu$ g/50  $\mu$ L of primary antibody [anti-CD31, anti-CD44, or anti-CD29 (BD Biosciences PharMingen); anti-ULEX (Vector Laboratories), anti-KDR (RELIAtech), or anti- $\alpha v\beta 3$  (Millipore)] for 1 h at 4 °C, followed by 1 h incubation with FITC-conjugated secondary antibodies (Santa Cruz). After extensive washes using FACS buffer, cells were analyzed at 488 nm on the flow cytometer FACScan system (BDFACSCanto).

### Cell adhesion assay

Sub-confluent cultures of ECPCs between the 3rd and 6th passage were used for the inhibition of adhesion assay. Plates (96 wells) were coated with Matrigel<sup>TM</sup> Matrix (BD

Biosciences) (10  $\mu$ g/ml), vitronectin (10  $\mu$ g/mL), fibronectin (1  $\mu$ g/mL), or osteopontin (0.5  $\mu$ g/mL), by overnight incubation at 4 °C. Plates were washed with PBS and then incubated at 37 °C for 1 h with PBS-1 % BSA. After being washed, ECPCs were counted, suspended in serum-free medium, and exposed to triazole RGD antagonists (final concentration was 0.01, 0.1, 1.0, or 10  $\mu$ M) at 37 °C for 30 min to allow for the ligand-receptor equilibrium to be reached. ECPCs were plated ( $(4-5)10^4$  cells/well) and incubated at 37 °C for 2 h. All the wells were washed with PBS to remove the non-adherent cells, and 0.5 % crystal violet solution in 20 % methanol was added. After 2 h of incubation at 4 °C, plates were examined at 540 nm in an ELX800 counter (Bio TEK Instruments). Data were expressed as percentage of inhibition compared to untreated cells. Experiments were conducted in triplicate and were repeated at least three times [49].

### RNA extraction and RT-PCR

Total RNA was extracted from ECPCs using RNeasy (Total RNA Isolation System, Promega, Madison, WI) and quantified spectrophotometrically. A volume of 500 ng of RNA was then retrotranscribed using ImProm-II reverse transcriptase (Promega, Madison, WI). Aliquots of 2  $\mu$ L of the cDNA were used for PCR amplification. The specific primers used for the identification of human  $\alpha v$ ,  $\beta 3$ , and GAPDH were designed according to published human cDNA sequences in the Genbank database, using FastPCR software [50]:  $\alpha v$  (forward 5'-CTA TGA GCT GAG AAA CAA TGG TCC-3' and reverse 5'-GCT GCT CCC TTT CTT GTT CTT C-3'/690-bp product);  $\beta 3$  (5'- GGG GAC TGCC TGT GTG ACT C-3' and reverse 5'-CTT TTC GGT CGT GGA TGG TG-3' 610-bp product); GAPDH (forward: 5'-ACC ACA GTC CAT GCC ATC AC-3' and reverse: 5'-TCC ACC ACC CTG TTG CTG TA-3', 452-bp product). PCR was carried out on a Perkin Elmer Thermal cycler. Ten microliters of each PCR products were visualized after electrophoresis in a 2 % agarose. cDNA products were evaluated on the basis of a standard PCR marker (Promega) and quantified by densitometric analysis using ImageJ software (NIH).

### Western blotting

ECPCs monolayers were lysed on ice in radioimmunoprecipitation assay buffer [50 mmol/L Tris-HCl (pH 7.5), 150 mmol/L NaCl, 1 % Triton X-100, 2 mmol/L EGTA, 1 mmol/L sodium orthovanadate, 1 mmol/L phenylmethane sulfonyl-fluoride, 10  $\mu$ g/mL aprotinin, and 10  $\mu$ g/mL leupeptin]. Samples were resolved by SDS-PAGE and transferred to a nitrocellulose membrane (Millipore, Billerica, MA). The blots were incubated in Blotk<sup>®</sup>-FL

blocking buffer at room temperature and probed with primary antibodies and appropriate secondary antibodies for infrared fluorescence detection. Membranes were visualized by Odyssey Imager which quantifies protein amount proportional to infrared signal. Antibodies used for western blotting were as follows: anti-TGF $\beta$ 1 (orb11468, Byorbit); anti- $\text{Alk5/TGF}\beta$ RI (GTX102784, Genetex); anti-PhosphoERK1/2 and anti ERK1/2 (9101 and 9102, Cell Signalling); anti  $\alpha$ -SMA (A2547, Sigma); anti-vimentin (V6630, Sigma); and anti-Phospho SMAD2 and anti-SMAD2/3 (3101 and 3102, Cell Signalling). Human anti- $\beta$ -tubulin (Millipore 05-661) was used as a loading control. Fluorescent goat anti-mouse and anti-rabbit secondary antibody were conjugated to AlexaFluor-680 and AlexaFluor-750, respectively (Invitrogen). Fluorescent signals of protein bands were recorded at 700 nm (mouse) and 800 nm (rabbit); in some experiments, the quantification of immunoblotting bands was performed by densitometric analysis with Odyssey infrared imaging system (LICOR Biosciences, USA).

### Immunofluorescence

ECPCs cells were cultured on 25-mm coverslips pre-coated with 10  $\mu\text{g/ml}$  of VN. After 24 h of incubation, in the presence of TGF $\beta$ 1, RGD-2 antagonist, or both, in complete EGM-2 medium, cells were washed in PBS, were fixed in 4 % paraformaldehyde, and membranes were permeabilized in 0.1 % Triton X-100 solution. Coverslips were incubated in blocking solution (PBS supplemented with 4 % BSA and 1 % horse serum) and then incubated at 4  $^{\circ}\text{C}$  overnight with anti- $\alpha$ -SMA primary antibodies, washed and incubated for 1 h with goat anti-mouse AlexaFluor-488 antibodies (Invitrogen). Cell nuclei were counterstained with DAPI (1  $\mu\text{g/ml}$  for 10 min at 37  $^{\circ}\text{C}$ ). Following two washes in PBS, coverslips were mounted with propylthiogallate on glass slides, and the cells were observed with an inverted confocal Nikon Eclipse TE2000 microscope equipped with a 960S-Fluor oil immersion lens.

### ECPCs migratory activity

In order to investigate the migratory activity of ECPCs, Boyden chamber assays were performed using Millicell cell culture inserts (Millipore 8- $\mu\text{m}$  pore size, 12 mm diameter). A 3D barrier of 50  $\mu\text{g/cm}^2$  of Matrigel was stratified on the filters, and ECPCs were loaded into the upper compartment ( $5 \times 10^4$  cells/well) in 400  $\mu\text{l}$  of complete EGM-2 containing TGF $\beta$ 1, RGD-2 antagonist, or both and placed into 24-well culture dishes containing 600  $\mu\text{l}$  of EGM-2 complete medium. After overnight incubation at 37  $^{\circ}\text{C}$ , non-invading cells were removed

mechanically using cotton swabs, and micro-porous membrane containing the invaded cells was fixed in 96 % methanol and stained with Diff-Quick staining solutions. Migratory activity was evaluated by counting the cells which migrated toward the lower surface of the filters (six randomly chosen fields for each filter).

### In vitro tube formation assay

The effects of TGF $\beta$ 1, RGD-2 antagonist, or both on the ability of ECPCs to reorganize and differentiate into capillary-like network were assessed, thereby Matrigel morphogenesis assay. Briefly, 50  $\mu\text{l}$  of Matrigel (1 mg/ml) was added into wells of a 96-well plate and polymerized for 1 h at 37  $^{\circ}\text{C}$ . After 24 h of incubation, in the presence of TGF $\beta$ 1, RGD-2 antagonist, or both, in complete EGM-2 medium, cells were washed once with PBS, harvested by trypsinization, and collected by centrifugation. Then, cells were resuspended in 200  $\mu\text{l}$  of EGM-2 complete medium and placed into Matrigel-coated wells ( $6 \times 10^5$  cells/well). After 12 h incubation on Matrigel at 37  $^{\circ}\text{C}$ , the plates were photographed under a phase contrast microscope. The degree of tubule formation was quantified by counting the branching points in four randomly chosen fields from each well [51].

### Wound healing assay

Cell migration was evaluated by an in vitro wound healing assay. Cells were grown at 80–90 % confluence in 35-mm dishes; the cell layer was wounded with a sterile 200- $\mu\text{l}$  pipette tip and incubated in 0.1 % FBS culture medium for 24 h. The wound was observed after 18 h, and pictures were taken using phase contrast microscope. The degree of healing was quantified by measuring the distance between opposing edges of the wound. Four wound/treatment and three measurements/wound were taken. Percentage of inhibition was expressed compared to untreated cells.

### Statistical analysis

Results were analyzed using a 2-tailed Student's *t* test to assess statistical significance. Statistical differences are presented at probability levels of  $P < 0.05$  or  $P < 0.01$ .

**Acknowledgments** This work was supported by Ministero dell'Istruzione, dell'Università e della Ricerca (MIUR, PRIN 2010–2011, Protocol No. 2010NRREPL\_006), the Istituto Toscano Tumori (ITT) (Grant No. 7197 29/12/2009), and Ente Cassa di Risparmio di Firenze (Protocol No. 2013.0688).

### Compliance with ethical standards

**Conflicts of interest** No potential conflicts of interest were disclosed.

**Open Access** This article is distributed under the terms of the Creative Commons Attribution 4.0 International License (<http://creativecommons.org/licenses/by/4.0/>), which permits unrestricted use, distribution, and reproduction in any medium, provided you give appropriate credit to the original author(s) and the source, provide a link to the Creative Commons license, and indicate if changes were made.

## References

- Rosenbloom J, Castro SV, Jimenez SA (2010) Narrative review: fibrotic diseases: cellular and molecular mechanisms and novel therapies. *Ann Intern Med* 152:159–166. doi:[10.7326/0003-4819-152-3-201002020-00007](https://doi.org/10.7326/0003-4819-152-3-201002020-00007)
- Klingberg F, Hinz B, White ES (2013) The myofibroblast matrix: implications for tissue repair and fibrosis. *J Pathol* 229:298–309. doi:[10.1002/path.4104](https://doi.org/10.1002/path.4104)
- Mayes MD (2003) Scleroderma epidemiology. *Rheum Dis Clin North Am* 29:239–254
- Pohlert D, Brenmoehl J, Löffler I, Müller CK, Leipner C, Schultze-Mosgau S et al (2009) TGF-beta and fibrosis in different organs—molecular pathway imprints. *Biochim Biophys Acta* 1792:746–756. doi:[10.1016/j.bbadis.2009.06.004](https://doi.org/10.1016/j.bbadis.2009.06.004)
- Wynn TA (2008) Cellular and molecular mechanisms of fibrosis. *J Pathol* 214:199–210
- Willis BC, duBois RM, Borok Z (2006) Epithelial origin of myofibroblasts during fibrosis in the lung. *Proc Am Thorac Soc* 3:377–382
- Hinz B, Phan SH, Thannickal VJ, Galli A, Bochaton-Piallat ML, Gabbiani G (2007) The myofibroblast: one function, multiple origins. *Am J Pathol* 170:1807–1816
- Piera-Velazquez S, Jimenez SA (2012) Molecular mechanisms of endothelial to mesenchymal cell transition (EndoMT) in experimentally induced fibrotic diseases. *Fibrogenesis Tissue Repair* 5(Suppl 1):S7. doi:[10.1186/1755-1536-5-S1-S7](https://doi.org/10.1186/1755-1536-5-S1-S7)
- Annes JP, Munger JS, Rifkin DB (2003) Making sense of latent TGFbeta activation. *J Cell Sci* 116:217–224
- Wipff PJ, Rifkin DB, Meister JJ, Hinz B (2007) Myofibroblast contraction activates latent TGF-beta1 from the extracellular matrix. *J Cell Biol* 179:1311–1323
- Hinz B (2013) It has to be the  $\alpha$ v: myofibroblast integrins activate latent TGF- $\beta$ 1. *Nat Med* 19:1567–1568. doi:[10.1038/nm.3421](https://doi.org/10.1038/nm.3421)
- Worthington JJ, Klementowicz JE, Travis MA (2011) TGF $\beta$ : a sleeping giant awoken by integrins. *Trends Biochem Sci* 36:47–54. doi:[10.1016/j.tibs.2010.08.002](https://doi.org/10.1016/j.tibs.2010.08.002)
- Asano Y, Ihn H, Yamane K, Jinnin M, Mimura Y, Tamaki K (2005) Increased expression of integrin  $\alpha$ (v) $\beta$ 3 contributes to the establishment of autocrine TGF-beta signaling in scleroderma fibroblasts. *J Immunol* 175:7708–7718
- Henderson NC, Sheppard D (2013) Integrin-mediated regulation of TGF $\beta$  in fibrosis. *Biochim Biophys Acta* 1832:891–896. doi:[10.1016/j.bbadis.2012.10.005](https://doi.org/10.1016/j.bbadis.2012.10.005)
- Margadant C, Sonnenberg A (2010) Integrin-TGF-beta crosstalk in fibrosis, cancer and wound healing. *EMBO Rep* 11:97–105. doi:[10.1038/embor.2009.276](https://doi.org/10.1038/embor.2009.276)
- Fabbrizzi P, Menchi G, Raspanti S, Guarna A, Trabocchi A (2014) Role of side-chain bioisosteres on the binding affinity of click chemistry-derived RGD peptidomimetics to  $\alpha$ v $\beta$ 3 integrin. *Eur J Org Chem* 2014:7595–7604. doi:[10.1002/ejoc.201403129](https://doi.org/10.1002/ejoc.201403129)
- Aota S, Nomizu M, Yamada KM (1994) The short amino acid sequence Pro-His-Ser-Arg-Asn in human fibronectin enhances cell-adhesive function. *J Biol Chem* 269:24756–24761
- Nagai M, Re S, Mihara E, Nogi T, Sugita Y, Takagi J (2012) Crystal structure of  $\alpha$ 5 $\beta$ 1 integrin ectodomain: atomic details of the fibronectin receptor. *J Cell Biol* 197:131–140. doi:[10.1083/jcb.201111077](https://doi.org/10.1083/jcb.201111077)
- Henderson NC, Sheppard D (2013) Integrin-mediated regulation of TGF $\beta$  in fibrosis. *Biochim Biophys Acta* 1832:891–896. doi:[10.1016/j.bbadis.2012.10.005](https://doi.org/10.1016/j.bbadis.2012.10.005)
- Shi Y, Massagué J (2003) Mechanisms of TGF-beta signaling from cell membrane to the nucleus. *Cell* 113:685–700
- Kang JS, Liu C, Derynck R (2009) New regulatory mechanisms of TGF-beta receptor function. *Trends Cell Biol* 19:385–394. doi:[10.1016/j.tcb.2009.05.008](https://doi.org/10.1016/j.tcb.2009.05.008)
- Goumans MJ, Valdimarsdottir G, Itoh S, Rosendahl A, Sideras P, ten Dijke P (2002) Balancing the activation state of the endothelium via two distinct TGF-beta type I receptors. *EMBO J* 21:1743–1753
- Sales VL, Engelmayr GC Jr, Mettler BA, Johnson JA Jr, Sacks MS, Mayer JE Jr (2006) Transforming growth factor-beta1 modulates extracellular matrix production, proliferation, and apoptosis of endothelial progenitor cells in tissue-engineering scaffolds. *Circulation* 114:1193–1199
- Pechkovsky DV, Scaffidi AK, Hackett TL, Ballard J, Shaheen F, Thompson PJ et al (2008) Transforming growth factor beta1 induces  $\alpha$ v $\beta$ 3 integrin expression in human lung fibroblasts via a  $\beta$ 3 integrin-, c-Src-, and p38 MAPK-dependent pathway. *J Biol Chem* 283:12898–12908. doi:[10.1074/jbc.M708226200](https://doi.org/10.1074/jbc.M708226200)
- Guo X, Wang XF (2009) Signaling cross-talk between TGF-beta/BMP and other pathways. *Cell Res* 19:71–88. doi:[10.1038/cr.2008.302](https://doi.org/10.1038/cr.2008.302)
- Lin F, Wang N, Zhang TC (2012) The role of endothelial-mesenchymal transition in development and pathological process. *IUBMB Life* 64:717–723. doi:[10.1002/iub.1059](https://doi.org/10.1002/iub.1059)
- Frid MG, Kale VA, Stenmark KR (2002) Mature vascular endothelium can give rise to smooth muscle cells via endothelial-mesenchymal transdifferentiation :in vitro analysis. *Circ Res* 90:1189–1196
- Piera-Velazquez S, Li Z, Jimenez SA (2011) Role of endothelial-mesenchymal transition (EndoMT) in the pathogenesis of fibrotic disorders. *Am J Pathol* 179:1074–1080. doi:[10.1016/j.ajpath.2011.06.001](https://doi.org/10.1016/j.ajpath.2011.06.001)
- Sheppard D (2005) Integrin-mediated activation of latent transforming growth factor  $\beta$ . *Cancer Metastasis Rev* 24:395–402
- Kim KL, Han DK, Park K, Song SH, Kim JY, Kim JM et al (2009) Enhanced dermal wound neovascularization by targeted delivery of endothelial progenitor cells using an RGD-g-PLLA scaffold. *Biomaterials* 30:3742–3748. doi:[10.1016/j.biomaterials.2009.03.053](https://doi.org/10.1016/j.biomaterials.2009.03.053)
- Trabocchi A, Menchi G, Cini N, Bianchini F, Raspanti S, Bottoncetti A et al (2010) Click-chemistry-derived triazole ligands of arginine-glycine-aspartate (RGD) integrins with a broad capacity to inhibit adhesion of melanoma cells and both in vitro and in vivo angiogenesis. *J Med Chem* 53:7119–7128. doi:[10.1021/jm100754z](https://doi.org/10.1021/jm100754z)
- Adamcic U, Skowronski K, Peters C, Morrison J, Coomber BL (2012) The effect of bevacizumab on human malignant melanoma cells with functional VEGF/VEGFR2 autocrine and intracrine signaling loops. *Neoplasia* 14:612–623
- Kharsaw M, Ameratunga MS, Grant R, Wheeler H, Pavlakis N (2014) Antiangiogenic therapy for high-grade glioma. *Cochrane Database Syst Rev* 9:CD008218. doi:[10.1002/14651858.CD008218](https://doi.org/10.1002/14651858.CD008218)
- Sargent DJ (2011) Chemotherapy: failure of bevacizumab in early-stage colon cancer. *Nat Rev Clin Oncol* 8:10–11. doi:[10.1038/nrclinonc.2010.205](https://doi.org/10.1038/nrclinonc.2010.205)
- Nisato RE, Tille JC, Jonczyk A, Goodman SL, Pepper MS (2003)  $\alpha$ v $\beta$ 3 and  $\alpha$ v $\beta$ 5 integrin antagonists inhibit angiogenesis in vitro. *Angiogenesis* 6:105–119

36. Scaringi C, Minniti G, Caporello P, Enrici RM (2012) Integrin inhibitor cilengitide for the treatment of glioblastoma: a brief overview of current clinical results. *Anticancer Res* 32:4213–4223
37. Ruffini F, Graziani G, Levati L, Tentori L, D'Atri S, Lacal PM (2015) Cilengitide down modulates invasiveness and vasculogenic mimicry of neuropilin 1 expressing melanoma cells through the inhibition of  $\alpha v \beta 5$  integrin. *Int J Cancer* 136:E545–E558. doi:[10.1002/ijc.29252](https://doi.org/10.1002/ijc.29252)
38. Reynolds AR, Hart IR, Watson AR, Welti JC, Silva RG, Robinson SD et al (2009) Stimulation of tumor growth and angiogenesis by low concentrations of RGD-mimetic integrin inhibitors. *Nat Med* 15:392–400. doi:[10.1038/nm.1941](https://doi.org/10.1038/nm.1941)
39. Bouvard C, Gafsou B, Dizier B, Galy-Fauroux I, Lokajczyk A, Boisson-Vidal C et al (2010) Alpha6-integrin subunit plays a major role in the proangiogenic properties of endothelial progenitor cells. *Arterioscler Thromb Vasc Biol* 30:1569–1575. doi:[10.1161/ATVBAHA.110.209163](https://doi.org/10.1161/ATVBAHA.110.209163)
40. Kim S, Bell K, Mousa SA, Varner JA (2000) Regulation of angiogenesis in vivo by ligation of integrin  $\alpha 5 \beta 1$  with the central cell-binding domain of fibronectin. *Am J Pathol* 156:1345–1362
41. de la Puente P, Muz B, Azab F, Azab AK (2013) Cell trafficking of endothelial progenitor cells in tumor progression. *Clin Cancer Res* 19:3360–3368. doi:[10.1158/1078-0432.CCR-13-0462](https://doi.org/10.1158/1078-0432.CCR-13-0462)
42. Caiado F, Dias S (2012) Endothelial progenitor cells and integrins: adhesive needs. *Fibrogenesis & Tissue Repair* 5:4. doi:[10.1186/1755-1536-5-4](https://doi.org/10.1186/1755-1536-5-4)
43. Rosenbloom J, Mendoza FA, Jimenez SA (2013) Strategies for anti-fibrotic therapies. *Biochim Biophys Acta* 1832:1088–1103. doi:[10.1016/j.bbadis.2012.12.007](https://doi.org/10.1016/j.bbadis.2012.12.007)
44. Henderson NC, Arnold TD, Katamura Y, Giacomini MM, Rodriguez JD, McCarty JH et al (2013) Targeting of  $\alpha v$  integrin identifies a core molecular pathway that regulates fibrosis in several organs. *Nat Med* 19:1617–1624. doi:[10.1038/nm.3282](https://doi.org/10.1038/nm.3282)
45. Akhurst RJ, Hata A (2012) Targeting the TGF $\beta$  signalling pathway in disease. *Nat Rev Drug Discov* 11:790–811
46. Woodcock HV, Maher TM (2014) The treatment of idiopathic pulmonary fibrosis. *F1000Prime Rep* 6:16. doi:[10.12703/P6-16](https://doi.org/10.12703/P6-16)
47. Bianchini F, Fabbrizzi P, Menchi G, Raspanti S, Bottoncetti A, Passeri A et al (2015) Radiosynthesis and micro-SPECT analysis of triazole-based RGD integrin ligands as non-peptide molecular imaging probes for angiogenesis. *Bioorg Med Chem* 23:1112–1122. doi:[10.1016/j.bmc.2014.12.065](https://doi.org/10.1016/j.bmc.2014.12.065)
48. Ingram DA, Mead LE, Tanaka H, Meade V, Fenoglio A, Mortell K et al (2004) Identification of a novel hierarchy of endothelial progenitor cells using human peripheral and umbilical cord blood. *Blood* 104:2752–2760
49. Margheri F, Chillà A, Laurenzana A, Serrati S, Mazzanti B, Saccardi R et al (2011) Endothelial progenitor cell-dependent angiogenesis requires localization of the full-length form of uPAR in caveolae. *Blood* 118:3743–3755. doi:[10.1182/blood-2011-02-338681](https://doi.org/10.1182/blood-2011-02-338681)
50. Kalendar R, Lee D, Schulman AH (2011) Java web tools for PCR, in silico PCR, and oligonucleotide assembly and analysis. *Genomics* 98:137–144. doi:[10.1016/j.ygeno.2011.04.009](https://doi.org/10.1016/j.ygeno.2011.04.009)
51. Parri M, Pietrovito L, Grandi A, Campagnoli S, De Camilli E, Bianchini F et al (2014) Angiopoietin-like 7, a novel pro-angiogenic factor over-expressed in cancer. *Angiogenesis* 17:881–896. doi:[10.1007/s10456-014-9435-4](https://doi.org/10.1007/s10456-014-9435-4)